LWT - Food Science and Technology 154 (2022) 112685

Contents lists available at ScienceDirect

LWT

journal homepage: www.elsevier.com/locate/lwt

Co-crystallized sucrose-soluble fiber matrix: Physicochemical and structural characterization

Marise Bonifácio Queiroz [a,*], Felipe Resende Sousa [b], Lidiane Bataglia da Silva [c], Rosa Maria Vercelino Alves [a], Izabela Dutra Alvim [d]

[a] Institute of Food Technology (ITAL), Av. Brasil, 2880, 13070-178, Campinas, SP, Brazil
[b] University of Campinas (UNICAMP), Faculty of Food Engineering, 13083-862, Campinas, SP, Brazil
[c] Fraunhofer Institute for Process Engineering and Packaging IVV, 85354, Freising, Germany
[d] Institute of Food Technology (ITAL), 13070-178, Campinas, SP, Brazil

ARTICLE INFO

Keywords:
Co-crystal
Dietary fiber
Sucrose
Resistant maltodextrin
Co-crystallization

ABSTRACT

Dietary fibers are often under-consumed worldwide, even though their health benefits are already established in dietary guidelines, which recommend their daily intake of 25–30 g. Increasing the supply of fiber-enriched food products is a way to improve consumers' daily intake. This study proposes the development of a mixed sucrose/erythritol/fiber matrix, particulate as a crystalline solid aggregate by the co-crystallization process to be used as a fiber-delivery ingredient in formulations with partial sugar reduction. The co-crystal was physicochemical and structurally characterized and compared to their individual components. The results indicated the formation of a sugar-based structure with fiber entrapped (29.8 g/100 g of co-crystals, db), presenting 5.33% of moisture content, 0,564 of water activity, and good flow properties. DSC thermogram displayed an endothermic transition peak at 187.31 °C, similar to the melting temperature of sucrose, suggesting the maintenance of the crystalline structure after co-crystallization and confirmed by X-ray diffraction and FTIR spectral profile. Morphological images showed small cluster agglomerates with a covering layer on structure, indicating the presence of the fiber in the matrix. Thus, co-crystallization constitutes an alternative process for the production of particulate crystalline solid containing fiber, being a great alternative to food ingredients in less sugar-added and fiber-enriched products.

1. Introduction

There is increasing consumer demand for additional dietary health benefits that go beyond basic nutrition. Fortified products with dietary fiber are growing in the global market and although it is a nutrient with a long history of scientific research on its physiological benefits, dietary fiber is often under-consumed in most countries around the world (Salmas, Devries, & Plank, 2017).

Evidence suggests that an adequate fiber intake maintains laxation, supports fecal bulking, and may decrease the risk of developing chronic diseases, such as cardiovascular disease, type 2 diabetes, and obesity (Burns et al., 2018). The most scientifically recognized effect of consuming dietary fiber is related to intestinal function (Bernaud & Rodrigues, 2013; McCleary, Sloane, & Draga, 2015).

Indigestible components found in starches (resistant starches) and in their hydrolyzed fractions (resistant dextrin and maltodextrin) present physiological functions of dietary fiber and make them suitable for use in several food formulations. One of the maltodextrins resistant, commercially available as Fibersol-2®, produced by a combination of hydrolysis and transglucosidation reactions has physiological attributes that resemble those of fiber, having well-developed, branched particles that are partially hydrolyzed by human digestive enzymes, with about 90% of its composition formed by these indigestible fractions (Ohkuma & Wakabayashi, 2000).

Resistant maltodextrin may attenuate the rise in serum glucose after a meal and has the potential to reduce peak postprandial blood glucose and insulin levels that are within the normal range in healthy individuals, besides increasing Bifidobacterium in the gut and satiety when consumed (Burns et al., 2018).

Sucrose co-crystallization is a process in which a food ingredient or

* Corresponding author.
E-mail addresses: bqueiroz@ital.sp.gov.br (M.B. Queiroz), felipesousa1496@live.com (F.R. Sousa), lidiane.bataglia@ivv-extern.fraunhofer.de (L.B. Silva), rosa@ital.sp.gov.br (R.M.V. Alves), izabela@ital.sp.gov.br (I.D. Alvim).

https://doi.org/10.1016/j.lwt.2021.112685
Received 19 July 2021; Received in revised form 18 October 2021; Accepted 21 October 2021
Available online 23 October 2021

mixtures of them are incorporated into a crystalline agglomerate of sucrose, through spontaneous sugar crystallization (Hartel, 2002). In the co-crystallization, the solid, dense, perfect crystal structure of sucrose changes to irregular agglomerated crystals with a sponge-like appearance with increased void space and surface area, thus providing a porous matrix in which another components can be incorporated (Karangutkar & Ananthanarayan, 2020).

A great deal of research has reported the use of co-crystallization to drive the encapsulation process, whereby properties such as solubility, wettability, hydration, homogeneity, dispersibility, anti-caking, and stability of the encapsulated materials can be improved (Sardar & Singhal, 2013; Beristain, Vazquez, Garcia, & Vernon-Carter, 1996; López-Córdoba, Gallo, Bucalá, Martino, & Navarro, 2015; Sarabandi, Mahoonak, & Akbari, 2019; Federzoni, Alvim, Fadini, da SILVA, & Queiroz, 2019; Kaur, Elsayed, Subramanian, & Singh, 2021). Moreover, the process offers direct tableting characteristics, an important property for the confectionery and pharmaceutical industries and it is a means to convert liquid ingredients/extracts containing active components to powdered form (Irigoiti, Yamul, & Navarro, 2021; Quast, Farina, Quast, Vieira, & Queiroz, 2020).

López-Córdoba and Navarro (2018) suggest that the agglomerates obtained by co-crystallization can be used as sugar-based ingredients in food formulations such as chocolates, mints, chewing gum, toffees, fudges, and also as a pharmaceutical excipient for direct compression.

In this study, the approach of co-crystallization was proposed to produce a mixed sucrose/erythritol/fiber matrix, particulate as a crystalline solid aggregate to be used in food formulations with partial sugar reduction as a delivery system of fiber.

The aggregation of individual components, forming a crystalline solid, proposes advantages for modifying their technological functional properties, such as flowability, compressibility, caking, dispersibility, and solubility in the application system and also for delivering fiber as a healthy nutrient in a sugar-reduced matrix with possibility of improving texture properties of the final products. Furthermore, the physico-chemical and detailed structural characterization of the co-crystallized matrix was performed to elucidate possible cause and effect relationships of its application in food systems.

2. Material and methods

2.1. Materials

Sucrose (SUC, Crystal Sugar Guarani, Tereos), erythritol powder (ERY, Zerose™ Erythritol STD GRAN, Cargill) and resistant maltodextrin as a fiber source (RMF, Fibersol-2™, ADM – 89.1 g/100 g total dietary fiber) were used in the formation of the co-crystallized mixed matrix.

2.2. Preparation of the co-crystallized mixed matrix

A co-crystallized matrix (CCM) was prepared as described by Federzoni et al. (2019), with modifications. The process is illustrated in Fig. 1, where briefly sucrose (45 g/100 g), erythritol (5 g/100 g), and distilled water (23 g/100 g) were preheated in a stainless steel pan (atmospheric conditions) to 119 °C, and then transferred to a hot plate (509D-1, Fisatom, Brazil). The syrup reached the final temperature of 123 °C, ranging from 0.5 to 1.0 °C/min (Datalogger 176 T4, Testo, Germany) and was cooled by using a vertical stirrer (TEC039/1, Tecnal, Brazil) (150 rpm/3 min in atmospheric conditions) to slight turbidity of the sucrose/erythritol syrup, indicating the beginning of the crystallization process. In the next step, the fiber (27 g/100 g) was added under stirring (150 rpm/2min. and 400 rpm/1 min). The co-crystallized matrix (CCM) was dried at 45 °C/4 h in a forced air convection oven (K13964, Proctor & Schwartz, USA), and the agglomerated was reduced to a powder with a knife grinder (Treu S.A., Brazil). The powder was sieved and the fraction retained (1.41 and 0.6 mm) was used.

Total dietary fiber (high and low molecular weight dietary fibers) was quantified by the AOAC 2001.03 method, with modifications. The sample was gelatinized with alpha-amylase and digested with enzymes to break down starch and protein. Ethanol was added to precipitate the soluble fiber. The sample was filtered; the filtrate was purified and then concentrated. Finally, the sample was analyzed by an HPLC system with refractive index detection (AOAC, 2005). Analysis performed in duplicate.

2.3. Characterization of materials and co-crystallized mixed matrix powder

The characterization of the individual materials (SUC, ERY, RMF), as well as the co-crystallized matrix (CCM), were performed. A control sample of recrystallized pure sucrose (RPS) was also produced as described in 2.2.

2.3.1. Moisture content, water activity (a_w) and sorption isotherm

Moisture content: volumetric Karl Fischer titration (Titrando 901, Methrom, Switzerland) with methanol: formamide solution (2:1, v/v) as solvent.

Water activity: electronic water activity meter (Chilled-Mirror Dewpoint System) at 25 °C (Acqua Lab series 4 model TEV, Decagon Devices Inc., USA).

Sorption isotherm: 1 g of sample in glass weighing bottle was subjected to different relative humidities (RH) within the range of 11.3–90.3% until equilibrium. Saturated salt solutions were used such as LiCl, $CaCO_3$, $MgCl_2$, K_2CO_3, $Mg(NO_3)_2$, KI, NaCl, KCl, and $BaCl_2$ (ASTM E104-02, 2012; Zimeri & Kokini, 2002). For the stabilization of samples weight, the desiccators were maintained at 25 ± 2.0 °C for 36 days, with initial and final weighing. The equilibrium moisture content was obtained through the difference between the sample weight after reaching equilibrium and its dry mass. The experimental data were fitted to some classical mathematical models for moisture sorption predictions (GAB, BET, Henderson, and Halsey), employing the *Excel*® software. The generalized reduced gradient method from the *Excel Solver* was performed to estimate the model parameters. In order to evaluate the goodness of the curve fitting, the determination coefficients of regression (R^2) and the minimum percent root mean square error (*%RMSE*) were provided (Suhag, Nayik, & Nanda, 2018).

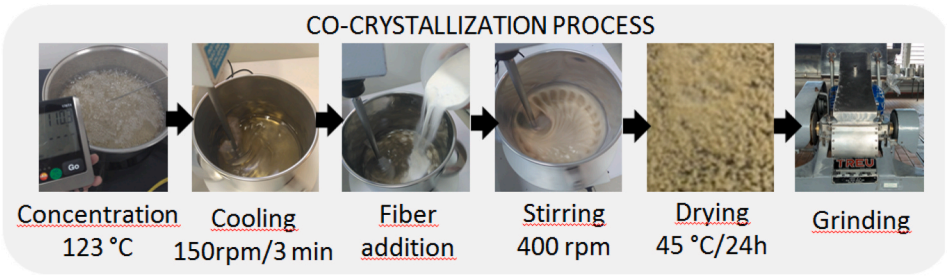

Fig. 1. Production of mixed matrix sucrose/soluble fiber by the co-crystallization process.

2.3.2. Dissolution kinetics (solubility)

The dissolution kinetics were determined by delivering a known mass of sample (10 g) into 100 mL of distilled water at 25 °C with continuous magnetic stirring at 270 rpm. Aliquots were removed at different times and the dissolved mass in the solution was determined using a refractometer (Q767BD Quimis, Abbe, Brazil) until the solution reached equilibrium in its refractive index (Sardar & Singhal, 2013; Federzoni et al., 2019; Kaur et al., 2021).

2.3.3. Bulk and tapped density

Bulk density (ρ_B) was evaluated by measuring the volume of 30 g of sample deposited freely by gravity into a 250 mL graduated cylinder. The tapped density (ρ_T) was calculated from the weight and volume occupied in the cylinder after being hand tapped until a constant value was reached. Both densities were determined by dividing the mass by the volume (Astolfi-Filho, Souza, Reipert, & Telis, 2005; López-Córdoba et al., 2015). Carr Index (CI) and Hausner Ratio (HR) were calculated according to equations (1) and (2), which are used as indicative of the flow capacity and the powder cohesiveness, respectively. CI is also used to represent powder compressibility, where higher values indicate low flow capacity and high compressibility (Aziz et al., 2018).

$$CI = (\rho_T - \rho_B)/\rho_T \times 100 \quad \text{Eq.01}$$

$$HR = \rho_T/\rho_B \quad \text{Eq.02}$$

2.3.4. Differential scanning calorimetry (DSC)

The thermal behavior was performed using a DSC (Discovery 250, TA Instruments, USA). The samples (4–8 mg) were placed in aluminum hermetic pans (Tzero) and heated at 10 °C/min from 25 to 200 °C in a nitrogen atmosphere. A modification of the methodology was also made for fiber (RMF) and co-crystallized matrix (CCM), using temperature modulation (MDSC) with heat flow at a rate of 3 °C/min.

2.3.5. X-ray diffraction (X-RD)

X-ray diffractograms were recorded at 2θ between 5° and 50° at 1.8°/min and step of 0.003° in an X´ Pert-MPD diffractometer (Philips Analytical, Netherlands), operated at 40 KV with radiation of wavelength of 40 mÅ, CuKα radiation with λ = 1,54056 Å.

2.3.6. Fourier transform infrared spectroscopy (FTIR)

The samples were scanned using Fourier Transform Infrared Spectrometer (Nicolet 6700, Thermo Scientific, USA). The spectra were recorded in transmission mode from 400 to 4000 cm^{-1} at a resolution of 4 cm^{-1}, 32 scans, and Snap-in Baseplate (KBr method).

2.3.7. Morphology (optical microscope and SEM)

Optical microscopy images were taken using a microscope (BX41, Olympus, Japan) fitted with a fiber optic light source (LGPS, Olympus, Japan) at a magnification of 100×. A digital camera (Q-color 3, Olympus America, USA) was attached to a microscope.

The surface morphology was observed by using a scanning electron microscope with X-ray dispersive energy detector (Leo 440i, LEO Electron Microscopy, England), with an accelerating voltage of 10 kV at magnifications of 150× and 700×. A layer of Au (200 Å estimated) was sputtered on the sample surface using a Sputter Coater (K450, Emitech, UK).

2.4. Data analysis

All sample measurements were carried out in triplicate and results are presented as mean ± standard deviation. Graphs were generated using excel and error bars in figures represent standard deviation. The one-way analysis of Variance (ANOVA) and Tukey HDS test was performed at a 95% confidence level using Statistica® 12 software to establish the statistical differences among means. Trios V.4.4 software was used to analyze the DSC results.

3. Results and discussion

3.1. Moisture content, water activity and sorption isotherm

Variable moisture content is observed depending on the nature of the material, being higher for RMF and lower for crystalline particles (SUC, RPS, and ERY) (Table 1). The increase in the moisture content when the sucrose is recrystallized is possibly due to the morphological change of the material with a consequent increase in the contact surface of the particulate structure and retention of a greater amount of adsorbed water.

Regarding water activity, the values were higher for crystalline sucrose particles compared to RMF (Table 1), but in all materials, they were considered low values (inferior to 0.612), showing no susceptibility to molds and yeasts growth (Ergun, Lietha, & Hartel, 2010). Sardar and Singhal (2013) found values of a_w of the pure sucrose crystal and pure co-crystallized sucrose equal or lower than 0.57, similar to results obtained in our study.

The crystalline particles have low moisture content and relatively higher water activity compared to the RMF, these being intrinsic characteristics of the materials. For SUC, this behavior is due to the nature of the crystalline structure with few pores where water can be bind (low moisture), but the water of surface is unbound, which increases the value of water activity. On the other hand, the fiber has a higher humidity due to the greater presence of pores or capillaries in the particle, this water being bound in the molecules through intermolecular interactions, which reduce the tendency to escape, as well as reducing its chemical potential with a consequent decrease in the water activity (Ergun et al., 2010).

The moisture sorption isotherms showed in Fig. 2 indicate that CCM was the most hygroscopic material, with low moisture absorption in water activity close to 0.58. On the other hand, ERY was the product that showed fewer changes in its visual characteristics with greater stability to the absorption of moisture at 25 °C. In general, GAB model showed a good fit to experimental data for SUC ($R^2 = 0.996$; %RMSE = 4.080) and RMF ($R^2 = 0.997$; %RMSE = 1.899), Henderson model for RPS ($R^2 = 0.998$; %RMSE = 2.352) and Halsey model for CCM ($R^2 = 0.997$; %RMSE = 10.187. ERY did not fit well in any of the evaluated models.

3.2. Dissolution kinetics (solubility)

The dissolution kinetics of materials and co-crystallized matrix are presented in Fig. 3. It was observed that the dissolution time of CCM was

Table 1
Results of moisture content, water activity (a_w), bulk (ρ_B) and tapped density (ρ_T), Carr index (CI) and Hausner ratio (HR) of raw materials and co-crystallized matrix.

Material	Moisture content (%)	a_w	ρ_B (g/cm^3)	ρ_T (g/cm^3)	CI (%)	HR
SUC	0.55 ± 0.01^c	0.540 ± 0.010^c	0.9327 ± 0.0083^a	0.9476 ± 0.0175^a	1.6^b	1.02^b
RPS	1.00 ± 0.10^c	0.612 ± 0.002^a	0.5888 ± 0.0004^c	0.6100 ± 0,0040^c	3.7^b	1.04^{ba}
ERY	0.32 ± 0.02^c	0.370 ± 0.010^e	0.8492 ± 0.0137^b	0.8697 ± 0.0126^b	2.4^b	1.02^b
RMF	6.75 ± 0.06^a	0.454 ± 0.007^d	0.4739 ± 0.0113^e	0.5143 ± 0.0051^e	8.6^a	1.09^a
CCM	5.33 ± 0.03^b	0.564 ± 0.005^b	0.5326 ± 0.0050^d	0.5709 ± 0.0330^d	8.5^a	1.09^a

Abbreviations: SUC, sucrose; RPS, recrystallized pure sucrose; ERY, erythritol; RMF, resistant maltodextrin (fiber); CCM, co-crystalized matrix. Values followed by different letters in the same column are significantly different ($P < 0.05$) according to Tukey's test.

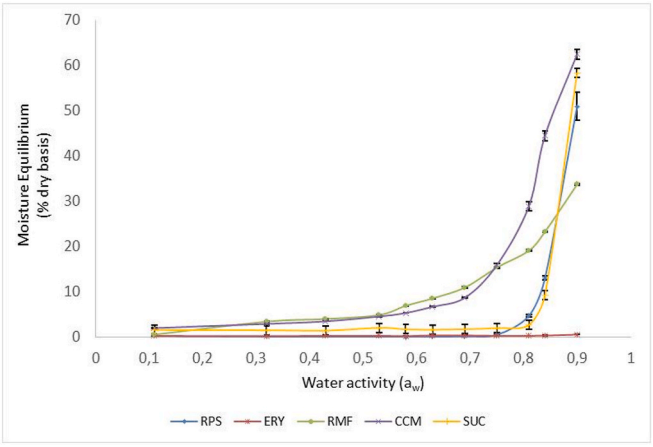

Fig. 2. Moisture sorption isotherms of sucrose (SUC), erythritol (ERY), recrystallized pure sucrose (RPS), resistant maltodextrin/fiber (RMF), and co-crystallized matrix (CCM) at 25 °C. Error bars representing standard deviation.

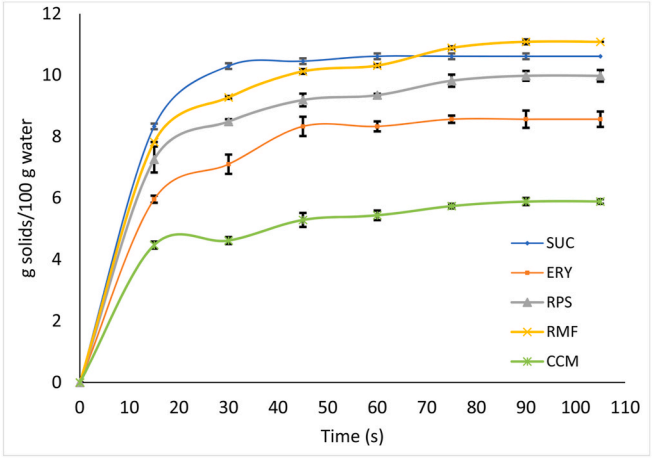

Fig. 3. Dissolution kinetics of sucrose (SUC), erythritol (ERY), recrystallized pure sucrose (RPS), resistant maltodextrin/fiber (RMF) and co-crystallized matrix (CCM) at 25 °C. Error bars representing standard deviation.

relatively higher than all other materials (SUC, ERY, and RMF) as well as the RPS. Sardar and Singhal (2013) reported a higher dissolution time of co-crystallized sucrose cubes compared to pure crystal sucrose and attributed this result to factors such as size, shape, and degree of crystallinity of the particles. Kaur et al. (2021) also found the dissolution time of carotenoids encapsulated co-crystals relatively higher than the pure sucrose due to the presence of active material in the interstices of co-crystals.

3.3. Bulk and tapped density

According to Table 1, bulk density values were lower than tapped, as expected, and this is due to the accommodation of the particles when subjected to movement. The shape of the fiber, as well as its smaller size, contributed to a greater variation between bulk and tapped densities compared to other materials. On the other hand, SUC and ERY presented less variation between densities due to their more regular crystalline form. In addition to the shape and size of the particles, their granulometric distribution also interfered with their compaction. The empty space between the large particles can be filled by smaller particles, which results in an increase in density, as reported by Saifullah, Yusof, Chin, and Aziz (2016).

The Carr index and Hausner ratio showed values below 10% and 1.11 (Table 1), respectively, for all powders. Although the CI values are in the range between 0 and 10%, considered as excellent flowability, according to the European Pharmacopoeia (Lebrun et al., 2012), it is noted that the co-crystallization process tends to reduce the powder flowability, with an increase in the CI for RPS compared to SUC, even if not statistically different. Furthermore, this flow property seems to have been governed by the presence of fiber in the structure, since CCM reached a value significantly higher than RPS and without significant difference from RMF. On the other hand, a higher CI for CCM should improve the compressibility of the powder for tablet applications, for example.

3.4. Differential scanning calorimetry (DSC)

The thermograms for SUC, RPS, and ERY showed expected results, with endothermic peaks with melting temperatures (Tm, corresponding to the peak temperature) and melting enthalpy (ΔH) of: Tm = 190.3 °C/ΔH = 121.9 J/g, Tm = 188.3 °C/ΔH = 122.8 J/g and Tm = 123.0 °C/ΔH = 304.9 J/g, respectively (Fig. 4). The values are similar to those reported by Talja and Roos (2001) and Hurtta, Pitkänen, and Knuutinen (2004). A slight decrease in Tm of sucrose is observed when it passes from its crystalline solid state (SUC) to an aggregate of smaller crystals (RPS), but the melting enthalpy remains constant. In addition, the melting enthalpy of ERY is substantially higher than that found and reported for SUC.

It was observed a drop in the normalized heat flow between 40 and 120 °C for RMF, with the formation of an extensive and low-intensity peak, probably due to the evaporation of water weakly bound, as reported by Elnaggar, El-Massik, Abdallah, and Ebian (2010) for a DSC of regular maltodextrin. It is still observed other variations of enthalpy, one stands out close to 144 °C and the other as an endothermic peak of Tm = 165.13 °C. Evaluating the MDSC, it is possible to note that at 144 °C the transition may be related to an enthalpic recovery, since it appears in the reversible heat flow, but it is not identified in the non-reversible, and may not be associated with a Tg, for example. The endothermic transition, on the other hand, may be associated with the fusion of the crystalline glucose fraction present in the fiber composition (Hurtta et al., 2004).

Resistant maltodextrin can be characterized as an oligosaccharide with DE between 8 and 12.5 and average composition of DP1 = 1.5%, DP2 = 2.5%, DP3 = 4.0%, DP4-6 = 12.0% and DP7 + = 80.0%, and it differs from a regular maltodextrin in its structural composition not only due to a α (1 → 4) and α (1 → 6) glycosidic bonds, such as those present in native starch, but also due to α conversions (1 → 4) for random connections of α (1 → 2) and α (1 → 3), as well as fractions of β connections (Ohkuma & Wakabayashi, 2000). Considering it is a material composed of different saccharides with different degrees of polymerization, RMF characterization by DSC has limitations since thermal transitions can overlap and make it difficult to analyze the thermograms.

The CCM thermogram indicated an endothermic transition peak at 187.31 °C, very close to the Tm of SUC and RPS, suggesting the maintenance of the crystalline structure of SUC after co-crystallization. A thermal event was also observed, with a very wide peak starting at 128 °C and a maximum peak temperature of 146.74 °C, which is very tenuous in the reversible heat flow, probably indicating evaporation of water. The peak observed at 187.31 °C, also present in the reversible and non-reversible heat flows of the MDSC, can be confirmed as a melting peak, which, due to the temperature, indicates the presence of sucrose crystal.

The absence of a peak close to Tm of erythritol in the CCM thermogram suggests that it did not crystallize in the matrix, but it was mixed with the fiber within the structure. When there is a total or partial disappearance of thermal events (melting point) in DCS, corresponding to materials present in the system, it may be indicating that they were incorporated in the matrix (Ponce Cevallos, Buera, & Elizalde, 2010; Pralhad & Rajendrakumar, 2004).

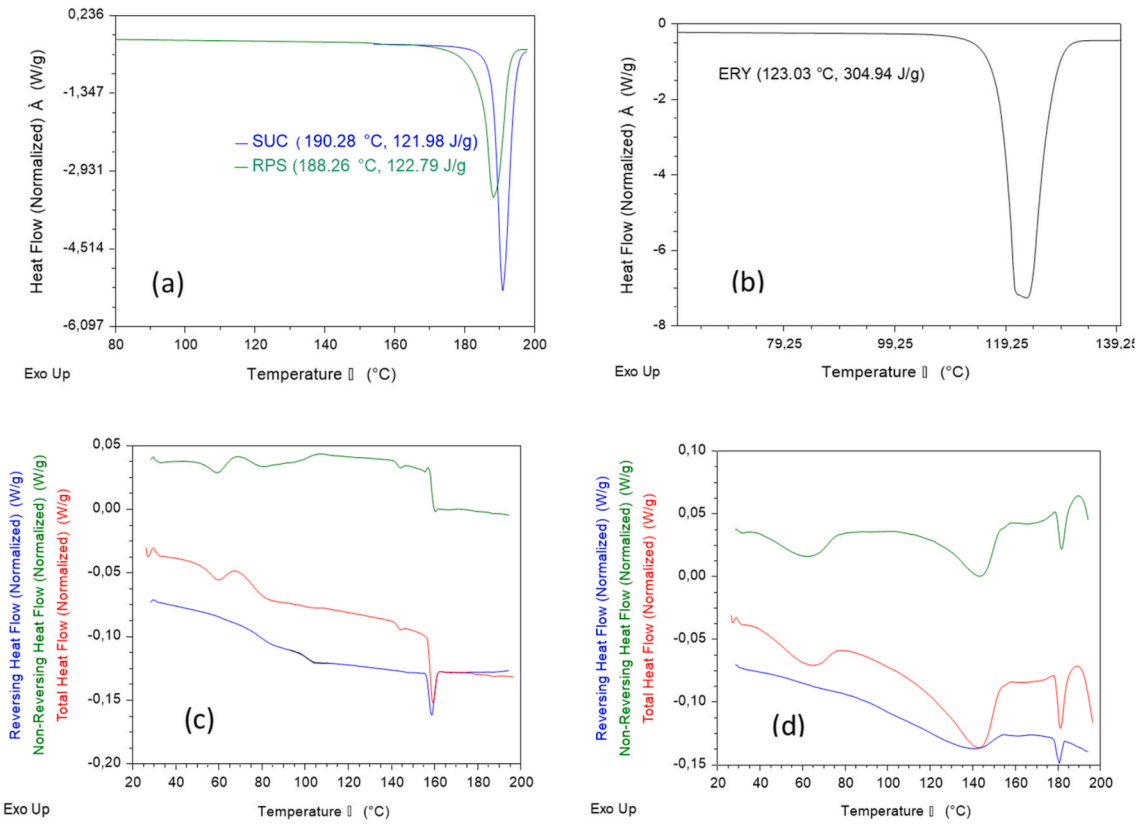

Fig. 4. DSC thermographs of (a) sucrose (SUC) and recrystallized pure sucrose (RPS), (b) erythritol (ERY); MDSC thermographs of (c) resistant maltodextrin/fiber (RMF), and (d) co-crystallized matrix (CCM).

3.5. X-RD

The X-ray diffractograms of all material are shown in Fig. 5. The two pure crystalline solids (SUC and ERY) showed characteristic diffraction patterns with several sharp peaks of greater intensity, suggesting high crystallinity for both (Pai, Vangala, Ng, Ng, & Tan, 2015; CHINACHOTI & STEINBERG, 1986). It was observed for SUC prominent peaks at angles (2θ) of 12.62°, 13.08°, 19.21°, 19.93°, 25.08°, 25.62° and 34.95°, similar to those found by López-Córdoba et al. (2015), Wongwiwat and Wattanachant (2014) and Sardar and Singhal (2013). For ERY, the highest intensity peaks appeared at angles (2θ) of 14.79°, 19.68°, 20.31°, 24.58°, 29.67°, 32.86°, and 42.73°.

On the other hand, RMF presented an expected pattern for amorphous materials, without defined peaks, the same behavior found for resistant wheat maltodextrin analyzed by Pai et al. (2015). Elnaggar et al. (2010) highlighted that the amorphous nature of maltodextrins is evident by the diffused or hollow structure X-ray pattern.

Comparing the diffraction patterns of SUC and RPS (12.75°, 13.12°,

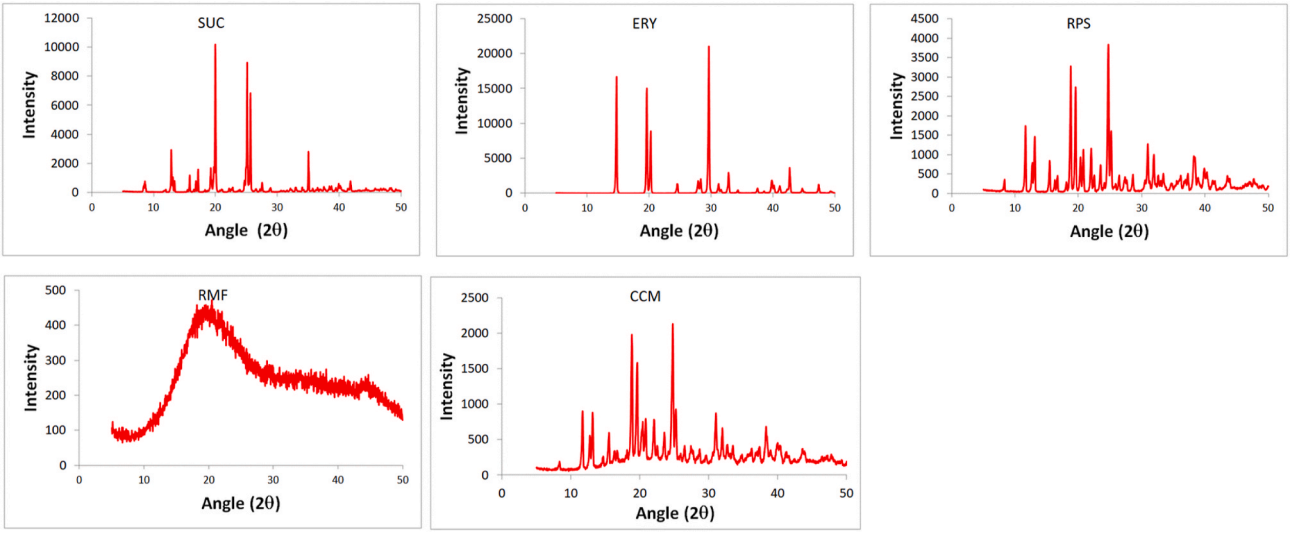

Fig. 5. X-ray diffraction patterns of sucrose (SUC), erythritol (ERY), recrystallized pure sucrose (RPS), resistant maltodextrin/fiber (RMF), and co-crystallized matrix (CCM).

18.79°, 19.56°, 20.79°, 24.72°, 25.17°, 30.96°, and 31.92°), a similar profile was noted, however, with peaks of lower intensity when the solid changes from a well-defined crystal to a crystalline cluster of small particles, suggesting a decrease in the crystallinity when there is a change in its physical structure.

Analyzing CCM diffractogram (11.71°, 12.76°, 13.17°, 18.85°, 19.65°, 24.78°, 25.23°, and 31.03°), it can be inferred that there was the formation of a crystalline structure similar to RPS with peaks of greater intensity in the same positions, indicating that the CCM has characteristics of a crystalline sucrose aggregate. A change in the baseline of the diffractogram was observed, with an upward displacement, mainly in the approximate angle of 20° (2θ), suggesting the presence of the fiber in the system, which can also be indicated by the decrease in the peak intensity or the crystallinity degree of the system due to its incorporation.

Regarding ERY in its pure form, the crystallinity was observed through very prominent peaks at 14.79°, 19.68°, 20.31°, 24.58°, 29.67°, 32.86°, and 42.73°, which intensity was larger than sucrose. However, it can be assumed that in the CCM, the crystalline structure of ERY was lost, being miscible in the matrix, since some peaks of greater intensity in its diffractogram did not appear in the diffractogram of the co-crystallized particle.

3.6. FTIR

The FTIR spectra for co-crystal individual components and for CCM are showed in Fig. 6. Both SUC and RPS presented similar and typical pattern as displayed in the spectral database for organic compounds (SDBS) (Matsuyama, Kinugasa, Tanabe, & Tamura, 2019) and observed by other authors (López-Córdoba et al., 2015; Santos, 2011, p. 117) regarding the "fingerprint" of sucrose. There is absorption attributed to the axial deformation of the –OH group involved in hydrogen bonding, originating three bands between 3600 and 3300 (3563 cm^{-1} - moderate intensity; 3388 cm^{-1} - wide and high intensity; 3337 cm^{-1} - low intensity). Between 3000 and 2800 cm^{-1} appeared characteristic C–H stretching vibration and in the range of 1200 to 700 cm^{-1} there were several bands of moderate intensity typical for carbohydrates, related to C–C bonds. The high intensity band observed at 1128 cm^{-1} suggests an association with C–O–C stretching vibration due to bond between fructose and glucose for the formation of sucrose, as demonstrated by Santos (2011), p. 117.

The spectral profile for ERY was also characteristic and in agreement with the SDBS (Matsuyama et al., 2019), showing vibrational bands of –OH in the range of 3500 to 3000 cm^{-1}, centered in 3263 cm^{-1}. Bands associated with C–C and C–O stretching vibrations appeared between 1300 and 600 cm^{-1}. Shen, Tan, Xu, and Guo (2017) highlight that erythritol also has two characteristic vibrational peaks, one at 1081 cm^{-1} generated by –OH (primary alcohol) and another at 1052 cm^{-1} corresponding to –OH (secondary alcohol). These peaks were also found in the ERY used to produce the CCM.

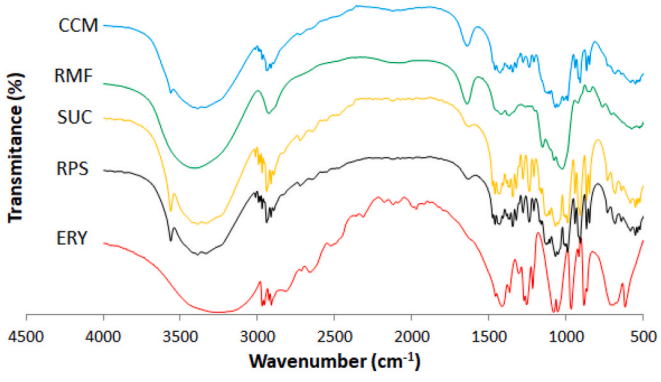

Fig. 6. FTIR spectra of sucrose (SUC), erythritol (ERY), recrystallized pure sucrose (RPS), resistant maltodextrin/fiber (RMF), and co-crystallized matrix (CCM).

Regarding the RMF spectra, absorption attributed to the axial deformation of the –OH group involved in hydrogen bonding was observed, originating a band in the range between 3500 and 3000 cm^{-1}, centered on 3405 cm^{-1}. Differently of other materials, RMF presented two peaks with vibrations in 2927 cm^{-1} and 1642 cm^{-1}, which according to Xie et al. (2018), it could be attributed to the C–H methylene groups of polysaccharides and to aromatic benzene, respectively, both found in soluble fibers of potato starch by-products. Peaks in these same positions are also found in the spectra of native starch and regular maltodextrin, showed in the SDBS (Matsuyama et al., 2019). Values with pronounced peaks between 1200 and 700 cm^{-1} can be attributed to the characteristic vibrational bands for carbohydrates (stretching of the C–O and C–C groups) and those specific in 1152, 1078 and 1025 cm^{-1} to the stretching of C–O–H, also found in resistant starch by Pérez-Masiá et al. (2015). According to the authors, bands around 923, 846 and 763 cm^{-1} could be attributed to the vibrations of the pyranose ring, specifically to the vibration of C–H elongation and glycosidic bonds α (1–6) and α (1–4) found in materials derived from starch.

Observing the spectral profile of CCM, it is noticed a mixture of the several overlapping spectral bands found in all the individual materials that composed the matrix and some specific to each material, indicating that the process was adequate to form a co-crystallized matrix with sucrose, erythritol, and fiber forming a particulate solid.

3.7. Morphology (optical and SEM images)

The optical and SEM images in Fig. 7 show the morphological difference of the materials and highlight some aspects of their structure. SUC and ERY displayed well-defined crystal structure with perfect surface edges for pure SUC and a nearly tetragonal structure for ERY, as reported by some authors (López-Córdoba et al., 2015; Rojas Mantilla, 2013; Sardar & Singhal, 2013; Tyapkova, Bader-Mittermaier, & Schweiggert-Weisz, 2012). RMF showed a different type of structure containing regular, smaller, and rounded particles, typical of spray drying particulate material. RPS exhibited a modified crystalline structure with small cluster-like agglomerates and void spaces with slightly sharper edges, similar to those found in co-crystals by Sardar and Singhal (2013), López-Córdoba, Deladino, Agudelo-Mesa, and Martino (2014) and López-Córdoba et al. (2015). CCM presented small cluster agglomerates as RPS, but without a well-defined edge. Comparing the images for both with a magnification of 700×, it is observed a slight modification in SUC crystallization behavior with the visualization of a covering layer on the structure of CCM, suggesting the presence of the fiber in the matrix. The crystals in the RPS are better defined and monoclinic, characteristic for this sugar.

The co-crystallized matrix resulted in a powder with 29.8 g/100 g of total dietary fiber, quantified in 11.9 g/100 g of high molecular weight dietary fiber and 17.9 g/100 g of low molecular weight dietary fiber, 5.33% of moisture content, and 64.9% of sucrose.

DSC/MDSC, X-RD, FTIR, and SEM techniques analyzed together allowed us to make some inferences about the structure of the co-crystallized powder. The DSC results showed an endothermic transition peak at 187.31 °C, confirmed by MDSC as a sucrose crystal melting peak and the X-RD exhibited a diffraction pattern with peaks of greater intensity at the same positions found in the SUC and RPS diffractograms. Furthermore, there was a disappearance of the thermal event at Tm close to the erythritol peak, as well as the absence of some peaks of greater intensity in the CCM diffractogram, suggesting its miscibility in the structure. Although materials composed of different saccharides with different degrees of polymerization, such as RMF, have limitations in characterization by DSC, the amorphous behavior of the fiber led to a change in the baseline of the diffractogram, indicating its presence in the matrix. A slight modification in the crystallization behavior of sucrose

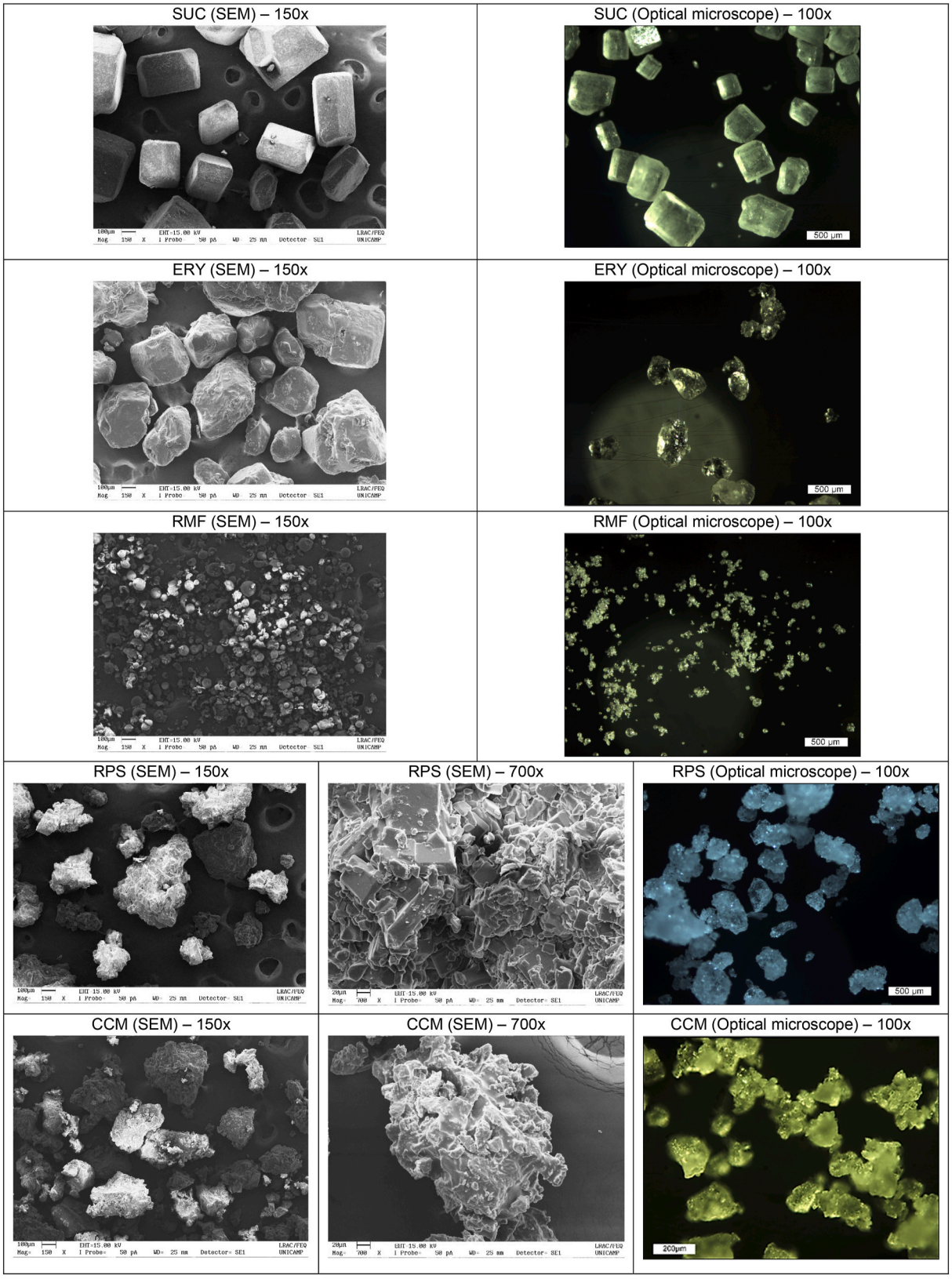

Fig. 7. Optical microscopy images and SEM micrographs of sucrose (SUC), erythritol (ERY), recrystallized pure sucrose (RPS), resistant maltodextrin/fiber (RMF), and co-crystallized matrix (CCM) at different magnifications.

with the visualization of a covering layer in the morphological structure of the co-crystal evidences the presence of the fiber also. The FTIR spectral profile presented a mixture of the several overlapping spectral bands found in all the individual materials that composed the matrix and some specific to each material, confirming the mixed composition of the product.

4. Conclusion

The co-crystallized mixed matrix powder showed characteristics of a sugar-based crystalline particulate material, with a reduction in sucrose and incorporation of 29.8 g/100 g, db of soluble fiber, desirable handling such as low water content and water activity, as well as good flow properties (flowability and compressibility).

Although fiber addition caused significant changes in physical and physicochemical properties, such as: moisture content, water activity, bulk and tapped density, and solubility, from a structural point of view, its presence was not able to change the crystalline behavior obtained by co-crystallization.

Structural characterization for the individual materials compared to the co-crystallized matrix was crucial to confirm the entrapment of the amorphous fiber in the sucrose crystal structure and the hypothesis of the formation of a mixed matrix composed of sucrose, erythritol and soluble fiber, through co-crystallization process.

Therefore, the developed co-crystal is a great alternative of food ingredient in products where fiber enrichment and sugar reduction are desired, with promising application in confectioneries (candies, jelly beans, tablets), bakeries (powder premixes) and also in hot and a cold powdered drink.

CRediT authorship contribution statement

Marise Bonifácio Queiroz: Conceptualization, Formal analysis, Funding acquisition, Investigation, Resources, Writing – original draft, editing. **Felipe Resende Sousa:** Investigation, Formal analysis, writing – figures editing. **Lidiane Bataglia da Silva:** Validation, Writing – review & editing. **Rosa Maria Vercelino Alves:** Methodology, Formal analysis. **Izabela Dutra Alvim:** Methodology, Formal analysis.

Declaration of competing interest

The author declare they have no known competing financial interests or personal relationships that could have appeared to influence the work reported in this paper.

Acknowledgements

The authors acknowledge to FAPESP by the financial support through project 2016/21930-4.

References

AOAC. (2005). *Official methods of analysis of the association of official analytical chemists* (18th ed.). Gaithersburg, MD: Association of Official Analytical Chemists.

ASTM E104-02. (2012). *Standard practice for maintaining constant relative humidity by means of aqueous solutions*. West Conshohocken, PA: ASTM International. www.astm.org.

Astolfi-Filho, Z., Souza, A. C., Reipert, É. C. D., & Telis, V. R. N. (2005). Encapsulação de suco de maracujá por co-cristalização com sacarose: Cinética de cristalização e propriedades físicas. *Ciência e Tecnologia de Alimentos, 25*(4), 795–801. https://doi.org/10.1590/s0101-20612005000400027

Aziz, M. G., Yusof, Y. A., Blanchard, C., Saifullah, M., Farahnaky, A., & Scheiling, G. (2018). Material properties and tableting of fruit powders. *Food Engineering Reviews, 10*(2), 66–80. https://doi.org/10.1007/s12393-018-9175-0

Beristain, C. I., Vazquez, A., Garcia, H. S., & Vernon-Carter, E. J. (1996). Encapsulation of orange peel oil by co-crystallization. *Lebensmittel-Wissenschaft und -Technologie- Food Science and Technology, 29*(7), 645–647. https://doi.org/10.1006/fstl.1996.0098

Bernaud, F. S. R., & Rodrigues, T. C. (2013). Fibra alimentar - Ingestão adequada e efeitos sobre a saúde do metabolismo. *Arquivos Brasileiros de Endocrinologia e Metabologia, 57*(6), 397–405. https://doi.org/10.1590/S0004-27302013000600001

Burns, A. M., Solch, R. J., Dennis-Wall, J. C., Ukhanova, M., Nieves, C., Mai, V., et al. (2018). In healthy adults, resistant maltodextrin produces a greater change in fecal bifidobacteria counts and increases stool wet weight: A double-blind, randomized, controlled crossover study. *Nutrition Research, 60*, 33–42. https://doi.org/10.1016/j.nutres.2018.09.007

Chinachoti, P., & Steinberg, M. P. (1986). Crystallinity of sucrose by X-ray diffraction as influenced by absorption versus desorption, waxy maize starch content, and water activity. *Journal of Food Science, 51*(2), 456–459. https://doi.org/10.1111/j.1365-2621.1986.tb11154.x

Elnaggar, Y. S. R., El-Massik, M. A., Abdallah, O. Y., & Ebian, A. E. R. (2010). Maltodextrin: A novel excipient used in sugar-based orally disintegrating tablets and phase transition process. *AAPS PharmSciTech, 11*(2), 645–651. https://doi.org/10.1208/s12249-010-9423-y

Ergun, R., Lietha, R., & Hartel, R. W. (2010). Moisture and shelf life in sugar confections. *Critical Reviews in Food Science and Nutrition, 50*(2), 162–192. https://doi.org/10.1080/10408390802248833

Federzoni, V., Alvim, I. D., Fadini, A. L., da Silva, L. B., & Queiroz, M. B. (2019). Co-crystallization of paprika oleoresin and storage stability study. *Food Science and Technology, 39*(June), 182–189. https://doi.org/10.1590/fst.41617

Hartel, R. W. (2002). Crystallization in foods. In *Handbook of industrial crystallization* (pp. 287–304). Elsevier. https://doi.org/10.1016/b978-075067012-8/50015-x.

Hurtta, M., Pitkänen, I., & Knuutinen, J. (2004). Melting behaviour of D-sucrose, D-glucose and D-fructose. *Carbohydrate Research, 339*(13), 2267–2273. https://doi.org/10.1016/j.carres.2004.06.022

Irigoiti, Y., Yamul, D. K., & Navarro, A. S. (2021). Co-crystallized sucrose with propolis extract as a food ingredient: Powder characterization and antioxidant stability. *Lebensmittel-Wissenschaft & Technologie, 143*, 111164. https://doi.org/10.1016/j.lwt.2021.111164. February.

Karangutkar, A. V., & Ananthanarayan, L. (2020). Co-crystallization of Basella rubra extract with sucrose: Characterization of co-crystals and evaluating the storage stability of betacyanin pigments. *Journal of Food Engineering, 271*, 109776. https://doi.org/10.1016/j.jfoodeng.2019.109776. October 2019.

Kaur, P., Elsayed, A., Subramanian, J., & Singh, A. (2021). Encapsulation of carotenoids with sucrose by co-crystallization: Physicochemical properties, characterization and thermal stability of pigments. *Lebensmittel-Wissenschaft & Technologie, 140*, 110810. https://doi.org/10.1016/j.lwt.2020.110810. August 2020.

Lebrun, P., Krier, F., Mantanus, J., Grohganz, H., Yang, M., Rozet, E., et al. (2012). Design space approach in the optimization of the spray-drying process. *European Journal of Pharmaceutics and Biopharmaceutics, 80*(1), 226–234. https://doi.org/10.1016/j.ejpb.2011.09.014

López-Córdoba, A., Deladino, L., Agudelo-Mesa, L., & Martino, M. (2014). Yerba mate antioxidant powders obtained by co-crystallization: Stability during storage. *Journal of Food Engineering, 124*, 158–165. https://doi.org/10.1016/j.jfoodeng.2013.10.010

López-Córdoba, A., Gallo, L., Bucalá, V., Martino, M., & Navarro, A. (2015). Co-crystallization of zinc sulfate with sucrose: A promissory strategy to render zinc solid dosage forms more palatable. *Journal of Food Engineering, 170*, 100–107. https://doi.org/10.1016/j.jfoodeng.2015.09.024

López-Córdoba, A., & Navarro, A. (2018). Physicochemical properties and stability of sucrose/glucose agglomerates obtained by cocrystallization. *Journal of Food Process Engineering, 41*(8), 13–18. https://doi.org/10.1111/jfpe.12901

Matsuyama, S., Kinugasa, S., Tanabe, K., & Tamura, T. (2019). Spectral database for organic compounds- SDBS. Retrieved from http://www.sdbs.db.aist.go.jp/. (Accessed 9 May 2019) Accessed.

McCleary, B. V., Sloane, N., & Draga, A. (2015). Determination of total dietary fibre and available carbohydrates: A rapid integrated procedure that simulates in vivo digestion. *Starch Staerke, 67*, 860–883. https://doi.org/10.1002/star.201500017

Ohkuma, K., & Wakabayashi, S. (2000). Fibersol-2: A soluble, non-digestible, starch-derived dietary fibre. In B. V. McCleary, & L. Prosky (Eds.), *Advanced dietary fibre technology*. https://doi.org/10.1002/9780470999615.ch44

Pai, D. A., Vangala, V. R., Ng, J. W., Ng, W. K., & Tan, R. B. H. (2015). Resistant maltodextrin as a shell material for encapsulation of naringin: Production and physicochemical characterization. *Journal of Food Engineering, 161*, 68–74. https://doi.org/10.1016/j.jfoodeng.2015.03.037

Pérez-Masiá, R., López-Nicolás, R., Periago, M. J., Ros, G., Lagaron, J. M., & López-Rubio, A. (2015). Encapsulation of folic acid in food hydrocolloids through nanospray drying and electrospraying for nutraceutical applications. *Food Chemistry, 168*, 124–133. https://doi.org/10.1016/j.foodchem.2014.07.051

Ponce Cevallos, P. A., Buera, M. P., & Elizalde, B. E. (2010). Encapsulation of cinnamon and thyme essential oils components (cinnamaldehyde and thymol) in β-cyclodextrin: Effect of interactions with water on complex stability. *Journal of Food Engineering, 99*(1), 70–75. https://doi.org/10.1016/j.jfoodeng.2010.01.039

Pralhad, T., & Rajendrakumar, K. (2004). Study of freeze-dried quercetin-cyclodextrin binary systems by DSC, FT-IR, X-ray diffraction and SEM analysis. *Journal of Pharmaceutical and Biomedical Analysis, 34*(2), 333–339. https://doi.org/10.1016/S0731-7085(03)00529-6

Quast, L. B., Farina, S. G., Quast, E., Vieira, M. A., & Queiroz, M. B. (2020). Co-crystallized honey with sucrose: Evaluation of process and product characterization. *Journal of Food Processing and Preservation, 44*(11), 1–9. https://doi.org/10.1111/jfpp.14876

Rojas, M. H. D. (2013). *Estudo da cristalização da sacarose com adição de antissolvente* (p. 177p). Dissretação (mestrado) - Universidade Federal de São Carlos.

Saifullah, M., Yusof, Y. A., Chin, N. L., & Aziz, M. G. (2016). Physicochemical and flow properties of fruit powder and their effect on the dissolution of fast dissolving fruit powder tablets. *Powder Technology, 301*, 396–404. https://doi.org/10.1016/j.powtec.2016.06.035

Salmas, G., Devries, J. W., & Plank, D. (2017). Challenges for dietary fiber: Benefits and costs of new U.S. regulations. *Cereal Foods World, 62*(3), 88–94. https://doi.org/10.1094/CFW-62-3-0088

Santos, L. B. (2011). *Caracterização Térmica de Sacarose de Cana-de-Açúcar: Amostras de Padrão de Referência, Comercial e Purificada*. Dissertação (mestrado) - Universidade Estadual Paulista, Instituto de Biociências, Letras e Ciências Exatas.

Sarabandi, K., Mahoonak, A. S., & Akbari, M. (2019). Physicochemical properties and antioxidant stability of microencapsulated marjoram extract prepared by co-crystallization method. *Journal of Food Process Engineering, 42*(1), 12949. https://doi.org/10.1111/jfpe.12949

Sardar, B. R., & Singhal, R. S. (2013). Characterization of co-crystallized sucrose entrapped with cardamom oleoresin. *Journal of Food Engineering, 117*(4), 521–529. https://doi.org/10.1016/j.jfoodeng.2012.12.011

Shen, S., Tan, S., Xu, G., & Guo, T. (2017). *The thermal properties of Erythritol/Adipic acid composite phase change material. 123* pp. 1226–1230). https://doi.org/10.2991/msmee-17.2017.231. Msmee.

Suhag, Y., Nayik, G. A., & Nanda, V. (2018). Modelling of moisture sorption isotherms and glass transition temperature of spray-dried honey powder. *Journal of food Measurement and Characterization, 12*, 2553–2560.

Talja, R. A., & Roos, Y. H. (2001). Phase and state transition effects on dielectric, mechanical, and thermal properties of polyols. *Thermochimica Acta, 380*(2), 109–121. https://doi.org/10.1016/S0040-6031(01)00664-5

Tyapkova, O., Bader-Mittermaier, S., & Schweiggert-Weisz, U. (2012). Factors influencing crystallization of erythritol in aqueous solutions: A preliminary study. *Journal of Food Research, 1*(4), 207. https://doi.org/10.5539/jfr.v1n4p207

Wongwiwat, P., & Wattanachant, S. (2014). Effect of sugar types on physical attributes and crystalline structure of sweet-dried chicken meat product. *International Food Research Journal, 21*(6), 2285–2291.

Xie, F., Zhang, W., Lan, X., Gong, S., Wu, J., & Wang, Z. (2018). Physicochemical properties and structural characteristics of soluble dietary fibers from yellow and purple fleshed potatoes by-product. *International Journal of Food Properties, 20*(3), S2939–S2949. https://doi.org/10.1080/10942912.2017.1387557

Zimeri, J. E., & Kokini, J. L. (2002). The effect of moisture content on the crystallinity and glass transition temperature of inulin. *Carbohydrate Polymers, 48*(3), 299–304. https://doi.org/10.1016/S0144-8617(01)00260-0